Electronic Supplementary Material (ESI) for Analyst.

Electronic Supporting Information

Exploring the Potential of a Urea Derivative: An AIE-Luminogen and Its Interaction with Human Serum Albumin in Aqueous Medium

Senjuti Halder, Soham Samanta and Gopal Das*

Department of Chemistry, Indian Institute of Technology Guwahati, Assam 781039, India.

Fax: + 91 361 258 2349; Tel: +91 361258 2313; E-mail: gdas@iitg.ernet.in

Table of Contents **Pages**

Experimental Section

General Information and Materials: Human Serum Albumin (HSA), Bovine Serum Albumin (BSA), DNA, DNase, Lysozyme, Cysteine, Pepsin, Trypsin, Ovalbumin, β-lactoglobulin, Pancreatin and all other materials for synthesis were purchased from commercial suppliers and used without further purification. Absorption measurements were carried out on a Perkin-Elmer Lamda-750 UV-Vis Spectrophotometer using 10 mm path length quartz cuvettes in the wavelength range of 250-700 nm, while the fluorescence spectra were recorded on a Horiba Fluoromax-4 Spectrofluorometer using 10 mm path length quartz cuvettes with a slit width of 3 nm at 298 K. Mass spectrum of $\mathbf{L_1}$ and $\mathbf{L_2}$ were obtained using Waters Q-ToF Premier mass spectrometer. Nuclear magnetic resonance (NMR) spectra were recorded on a Bruker Advance 600 MHz instrument. The chemical shifts were recorded in parts per million (ppm) on the scale. The following abbreviations are used to describe spin multiplicities in ^{1}H NMR spectra: s = singlet; d = doublet; t = triplet; q= quartet, m = multiplet.

Detection Limit: The detection limit was calculated on the basis of the fluorescence titration. The fluorescence emission spectrum of $\mathbf{L_1}$ was measured 10 times, and the standard deviation of blank measurement was estimated (λem = 438 nm). To measure the slope, the fluorescence emission at 438 nm was plotted as a function of the concentration of HSA from the titration experiment. The detection limit was then calculated using the following equation:

$$\text{Detection limit} = 3\sigma/k \qquad (1)$$

where σ is the standard deviation of blank measurement, and k is the slope between the fluorescence emission intensity versus [HSA].

Field Emission Scanning Electron Microscopy: FESEM imaging studies were conducted separately with a solution of $\mathbf{L_1}$ (1 mM) and $\mathbf{L_2}$ (1 Mm) by changing water fraction from 50% to 100% in CH_3CN-H_2O by drop (2 μl) cast method on glass plates covered with Al-foil using Gemini 300 FESEM (Carl Zeiss).

Fluorescence Microscopy: The samples [$\mathbf{L_1}$(10 μM) on increasing acetonitrile fraction up to 50% in water-acetonitrile mixture] were prepared freshly by casting all preparation drops(5 μl)

on a glass slide and were dried completely at room temperature followed by image acquisition using a fluorescence microscope (Eclipse Ti-U, Nikon, USA) with blue filter.

Transmission Electron Microscopy: The size and morphology of the $\mathbf{L_1}$-aggregates on increasing acetonitrile fraction in aqueous medium and $\mathbf{L_1}$ in presence of HSA in aqueous solution were determined by transmission electron microscopy (TEM) using a JEM-2100 (JEOL) microscope. The samples [$\mathbf{L_1}$(2μM) in 50% acetonitrile/water solution) , HSA (0.15 mg/mL), HSA(0.15 mg/mL)+$\mathbf{L_1}$(2μM) in water] were prepared freshly by casting one preparation drop (5 μl) on carbon coated copper grids and the sample was dried completely at room temperature and images were observed under TEM.

Dynamic light scattering studies: The particle sizes of $\mathbf{L_1}$, aggregated $\mathbf{L_1}$ and $\mathbf{L_1}$+HSA were measured by dynamic light scattering (DLS) experiments on Malvern Zetasizer Nano ZS instrument equipped with a 4.0 mW He–Ne laser operating at a wavelength of 633 nm. The samples and the background were measured at room temperature (25 °C). DLS experiments were carried out with optically clear solutions of $\mathbf{L_1}$ (2 μM) to observe the change in the particle size upon increasing the CH_3CN fraction. DLS studies were also carried out with an optically clear solution of $\mathbf{L_1}$ (2 μM) in water, in the presence and absence of HSA separately to determine the changes in the particle size on the interaction of L_1 with HSA. The solution was equilibrated for 60 minutes before taking the measurements.

Circular dichroism measurements: CD spectra of aqueous solutions of $\mathbf{L_1}$ (0.02 μM) , only HSA (15 μg/mL) and HSA in presence of $\mathbf{L_1}$ were recorded by using a 2 mL quartz cuvette of 10 mm path length with a J-1500 (Jasco) spectropolarimeter at room temperature. Spectra were collected at 1 nm intervals and 1 nm bandwidth from 190 to 450 nm.

FRET and REES study: In case of fluorescence measurement for FRET experiment, the donor HSA was excited at 295 nm and emission spectra were recorded 310–580 nm wavelength range. For REES experiment, the Trp was excited at both 295 and 310 nm to investigate the REES effect. The value of $\Delta\lambda_{em}^{max}$ is defined as the difference of the emission maximum obtained for the excitation wavelength at 295 nm and 310 nm,

Measurement of fluorescence lifetime: Fluorescence lifetimes were measured employing the time-correlated single-photon counting (TCSPC) method using Edinburgh Instrument Life-Spec II spectrometer. The samples ($\mathbf{L_1}$ and $\mathbf{L_1}$+HSA) were excited at 390 nm keeping the emission wavelength at 438 nm using a pulsed diode laser. The fluorescence decays were analyzed by the re-convolution method using the FAST software provided by Edinburgh Instruments.

Competitive Drug Displacement Study: It has been well established that serum proteins are composed of three homologous a-helical domains (I–III) and each domain contains two sub domains. The principal ligand binding sites of HSA are located in hydrophobic cavities in sub domains IIA and IIIA, which are referred to as site I and site II according to the terminology. To identify $\mathbf{L_1}$ binding site on HSA, site marker competitive experiments were carried out using three site-specific drugs comprising warfarin (domain IIA), ibuprofen (domain IIIA) and salicylic acid (a site marker of subdomains IIA & IB).

2.5. Molecular Docking Study: Molecular docking was conducted to analyze the geometrically and energetically stable conformation upon binding of probe $\mathbf{L_1}$ to HSA. AutoDockTools-1.5.6 was used to generate a docked conformation of $\mathbf{L_1}$ with HSA by employing a Genetic Algorithm (GA) and a Lamarckian Genetic Algorithm. The binding free energies and binding sites of $\mathbf{L_1}$ within the active site of HSA were examined by this software. The crystal structure of HSA with four letter codes (1BM0) was retrieved from RCSB PDB (Sugio, S., Kashima, A., Mochizuki, S., Noda, M., Kobayashi, K. *Protein Eng.* **1999**, *12*, 439-446), and was subject to energy refinement, hydrogen additions and solvent removal through Swiss PDB Viewer v.4.1.0 to allow all the residues to adopt a correct and stable configuration. To define all binding sites, a grid box was generated with a spacing of 0.375 °A and dimensions of (60x60x60) points (.gpf file). The docking parameters were inserted as the number of GA runs: 25. The output is selected as Lamarckian GA (.dpf file), which was applied in AutoDockTools-1.5.6 to conduct docking simulations. Energy minimization and optimization of the probe $\mathbf{L_1}$ was also performed. In the end, analysis of docking result of the probe $\mathbf{L_1}$ was done using PyMOL viewer programs and the docking structure with the lowest binding energy calculated by AutoDockTools-1.5.6 was selected as the best binding conformation.

Density Functional Theory (DFT) Study: DFT optimizations of $\mathbf{L_1}$ were carried out with the RB3LYP/ 6-31G method basis set using the Gaussian 09 program where calculated total energy is **-1148.25535936 a.u**.

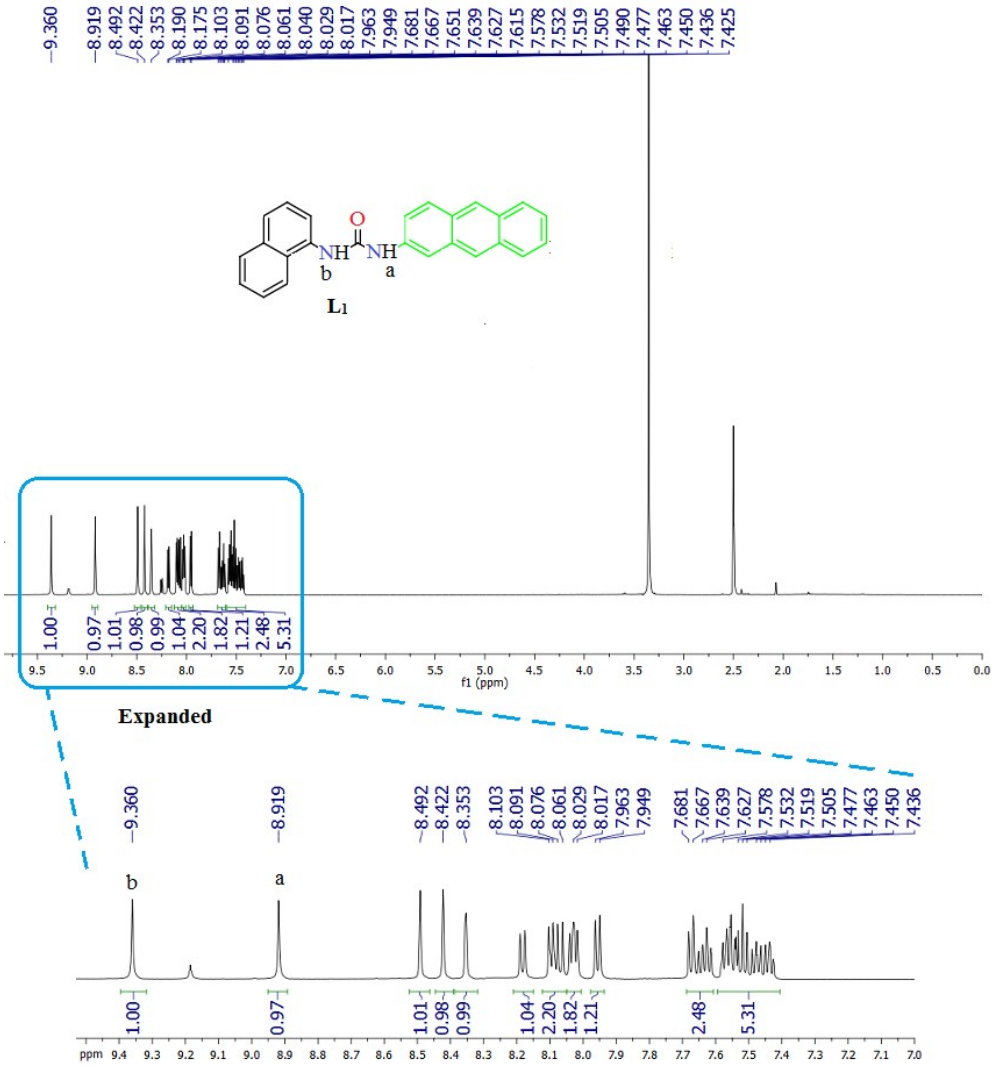

Figure S1: ^{1}H-NMR spectra of $\mathbf{L_1}$ in DMSO-d_6.

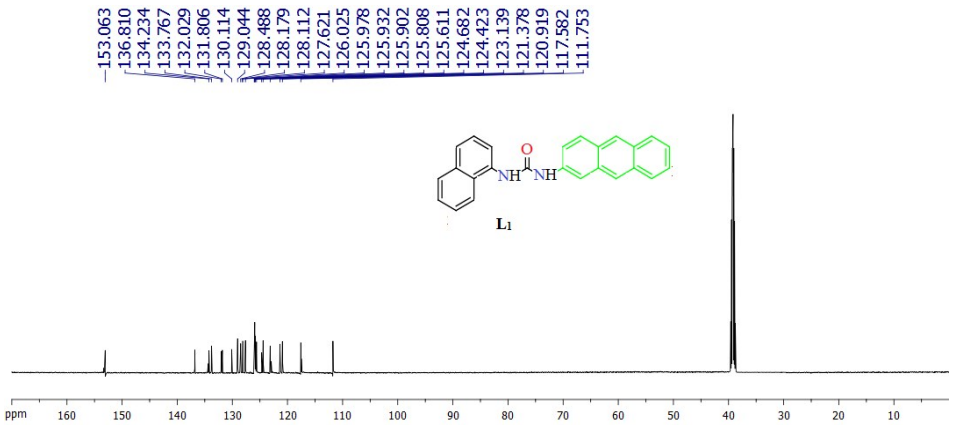

Figure S2: ^{13}C-NMR spectra of $\mathbf{L_1}$ in DMSO-d_6.

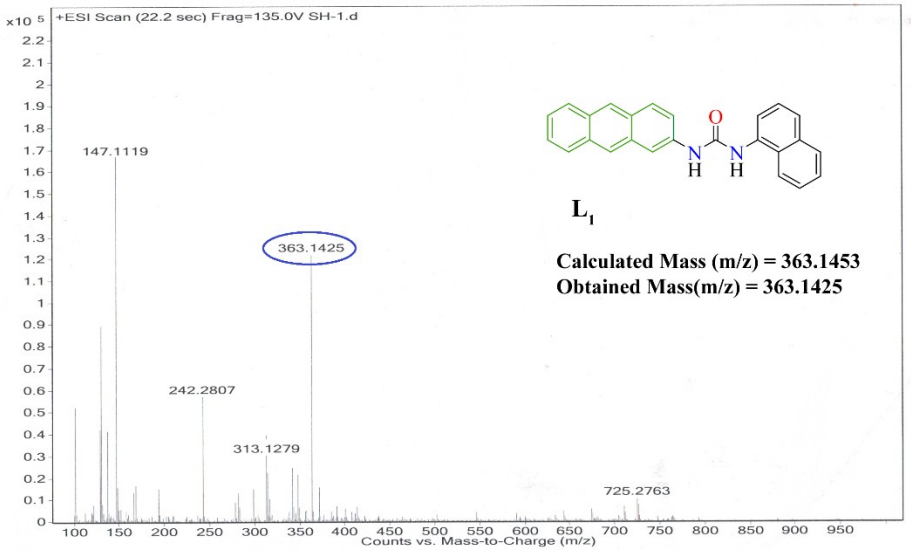

Figure S3a: Mass spectrum of $\mathbf{L_1}$.

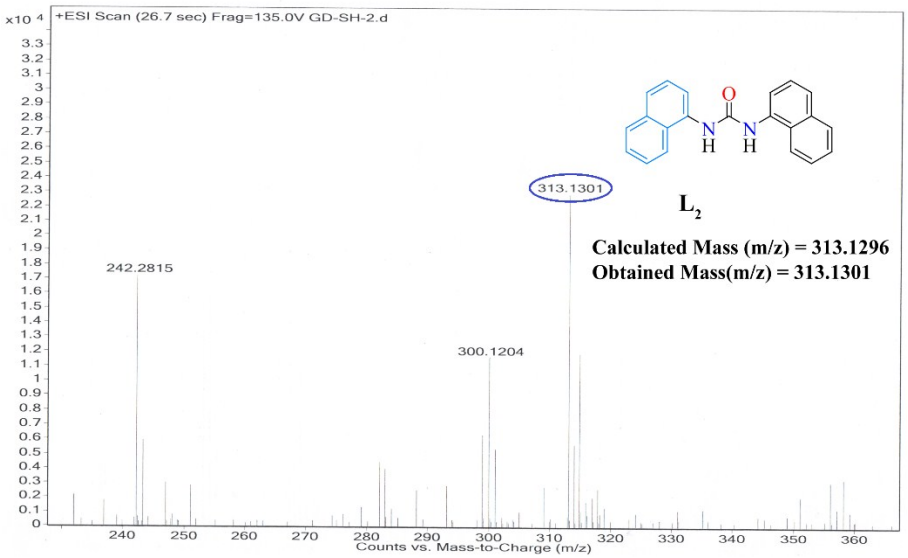

Figure S3b: Mass spectrum of $\mathbf{L_2}$.

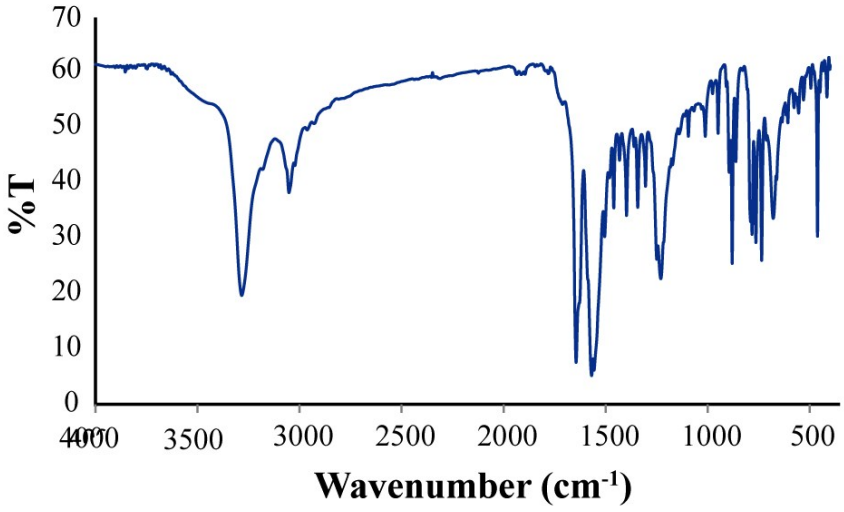

Figure S4: FT-IR spectrum of $\mathbf{L_1}$ recorded in KBr pellet at 25ºC.

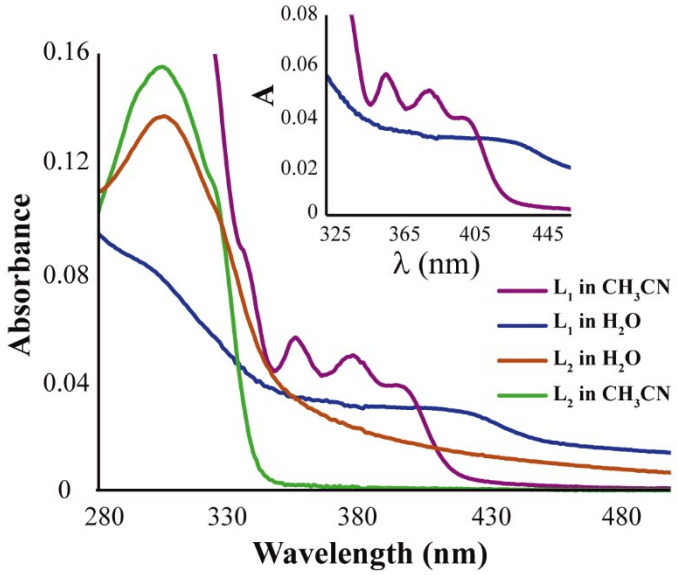

Figure S5: UV-Vis changes of $\mathbf{L_1}$ and $\mathbf{L_2}$ (10 μM) in various solvents at room temperature. INSET: Expanded region of the spectra in the wavelength region 325nm - 500 nm.

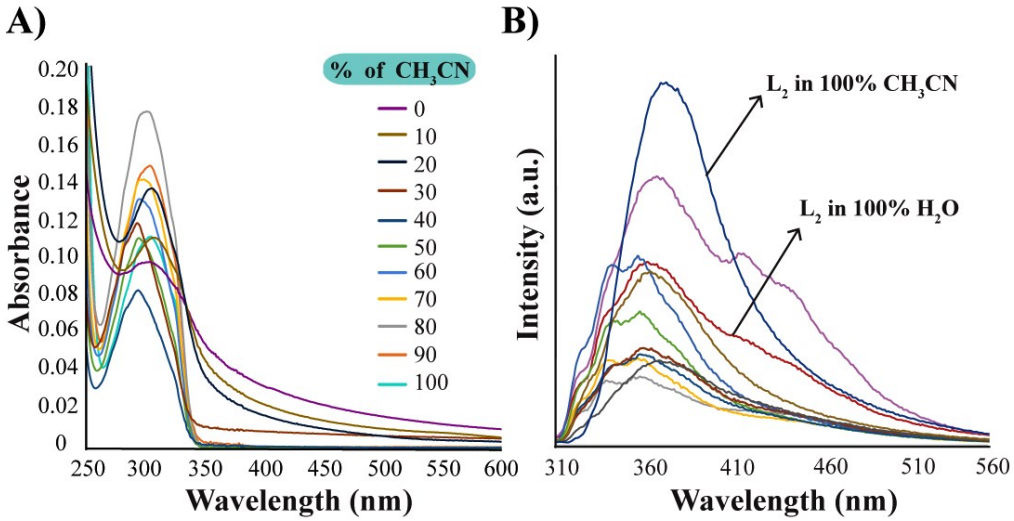

Figure S6: A) U-V Visible spectra of $\mathbf{L_2}$ (10 μM) in CH_3CN-H_2O with different CH_3CN fractions; B) Fluorescence spectra of $\mathbf{L_2}$ (2 μM) in CH_3CN-H_2O with different CH_3CN fractions (λ_{ex} = 300 nm);

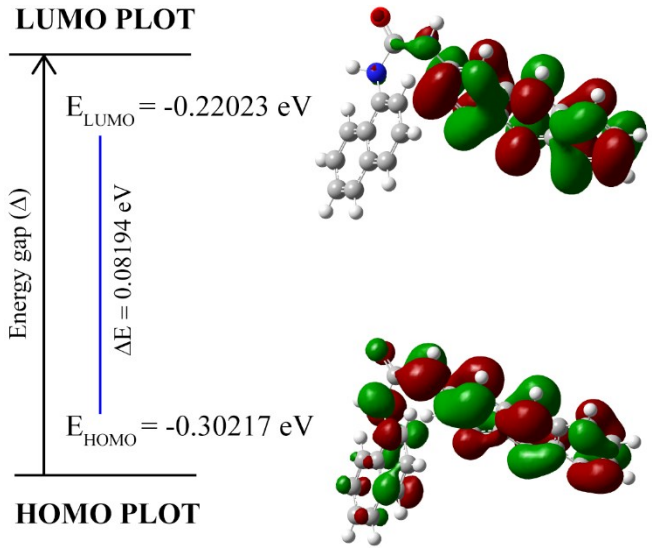

Figure S7: Frontier molecular orbital plots of $\mathbf{L_1}$ (ΔE = energy gap between HOMO and LUMO).

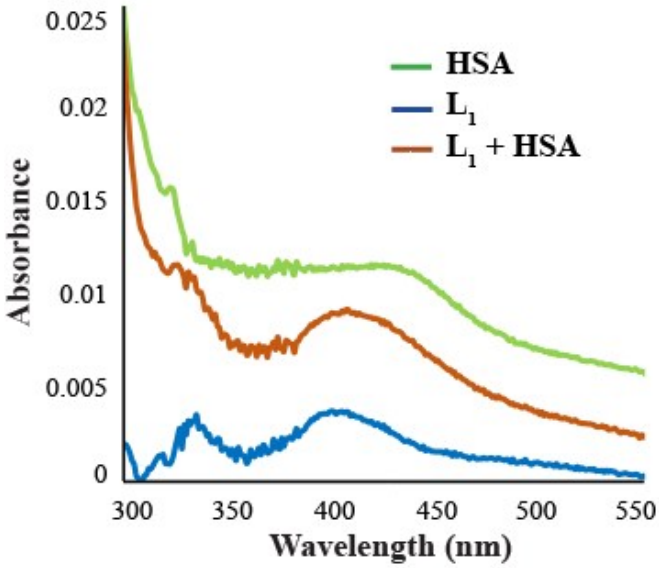

Figure S8: UV-visible spectra of $\mathbf{L_1}$ (2 μM) in aqueous medium in presence HSA (150 μg/mL).

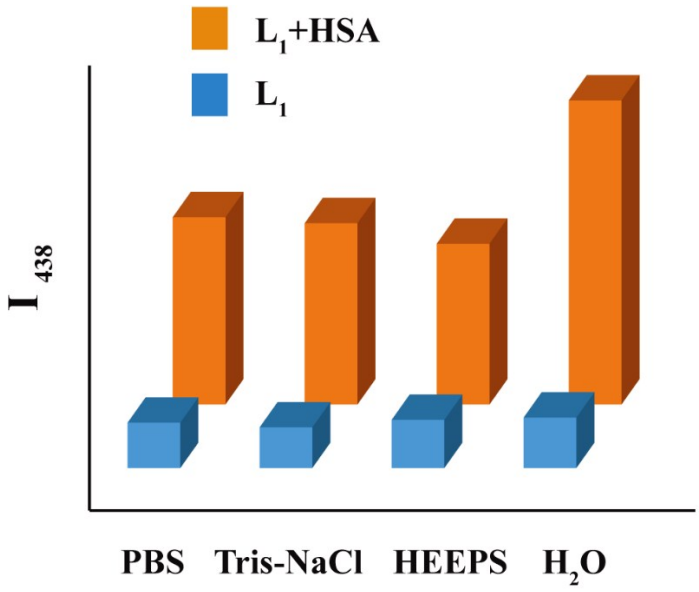

Figure S9: Fluorescence response of L_1 (2 μM) at 438 nm upon interaction with HSA (150 μg/mL) in different medium

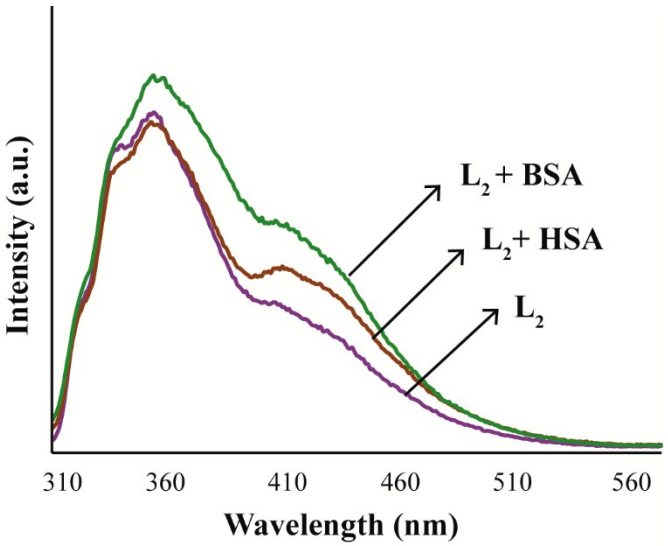

Figure S10: Fluorescence spectra of **L_2** (2 μM) in aqueous medium in presence of HSA and BSA(150 μg/mL).

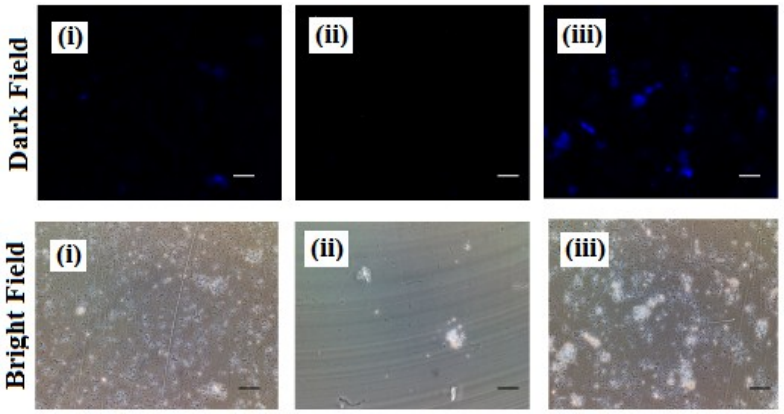

Figure S11: Fluorescence microscope images in 100% aqueous solution of (i) only $\mathbf{L_1}$ (ii) only HSA (iii) $\mathbf{L_1}$ in presence of HSA.

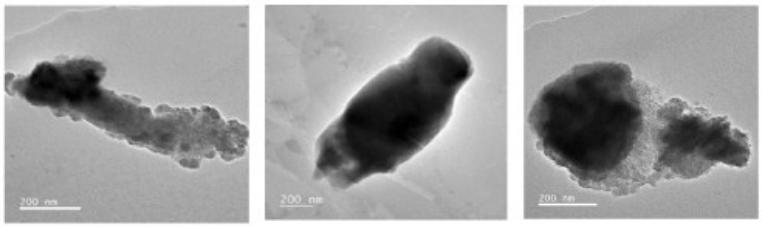

Figure S12: TEM images of the $\mathbf{L_1}$ in presence of HSA in 100% aqueous solution (scale bar = 200 nm).

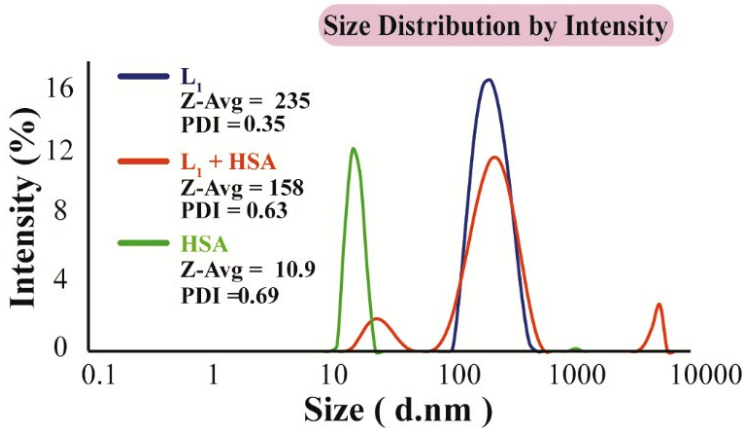

Figure S13: DLS-based particle size analysis; change in particle size of $\mathbf{L_1}$ (2 μM) in aqueous medium upon interaction with HSA (150 μg/mL).

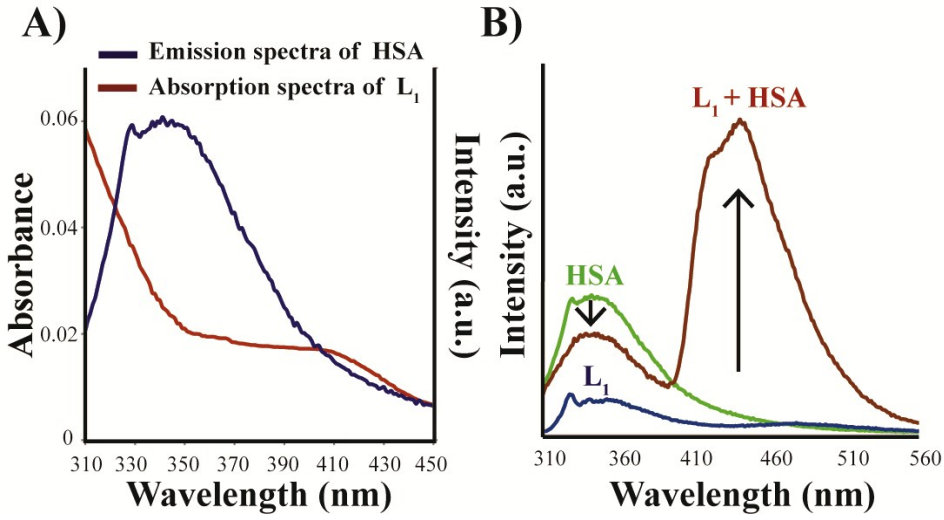

Figure S14: A) Spectral overlap of emission spectra of HSA and absorption spectra of $\mathbf{L_1}$; B) The occurrence of FRET with addition of $\mathbf{L_1}$ (2 μM) to HSA (150 μg/mL) in aqueous medium.

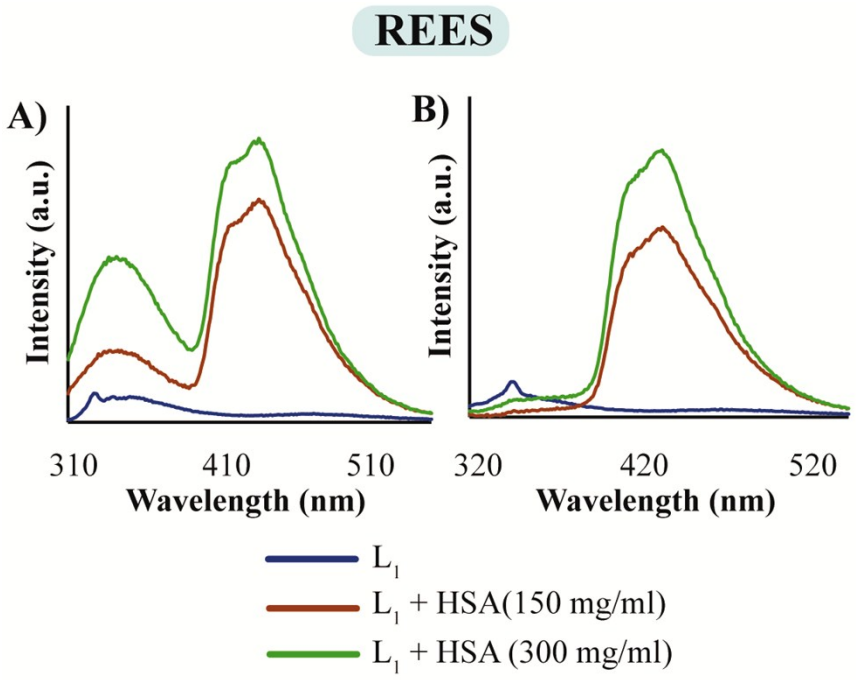

Figure S15: Red edge excitation shift effects at A) λ_{ex} 295 nm and B) λ_{ex} 310 nm.

Table S1: Red edge excitation shift effects at λ_{ex} 295 nm and at λ_{ex} 310 nm.

	λ_{em}^{max}		
Sample	**λex 295 nm**	**λex 310 nm**	**REES (nm)**
L_1	346	346	0
L_1+HSA (150 µg/mL)	344	349	5
L_1+HSA (300 µg/mL)	344	354	10

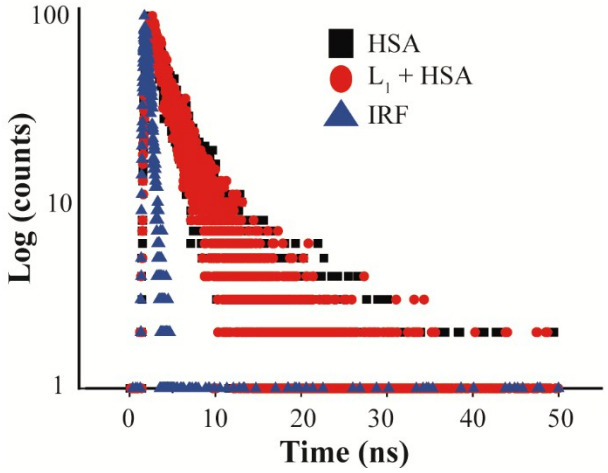

Figure S16: Fluorescence lifetime decay profiles of $\mathbf{L_1}$ (2 μM)in absence and in presence of HSA (150 μg/mL) in aqueous medium.

Table S2: Lifetime of $\mathbf{L_1}$ A) in the absence and B) in presence of HSA where $\langle\tau\rangle = a_1\tau_1 + a_2\tau_2$

Sample	B_1	B_2	a_1	a_2	τ_1	τ_2	$\langle\tau\rangle$	χ^2
$\mathbf{L_1}$	0.055	0.001	0.719	0.281	0.442	6.721	2.206	0.935
$\mathbf{L_1}$**+HSA**	0.008	0.004	0.198	0.801	1.528	14.290	11.749	1.233

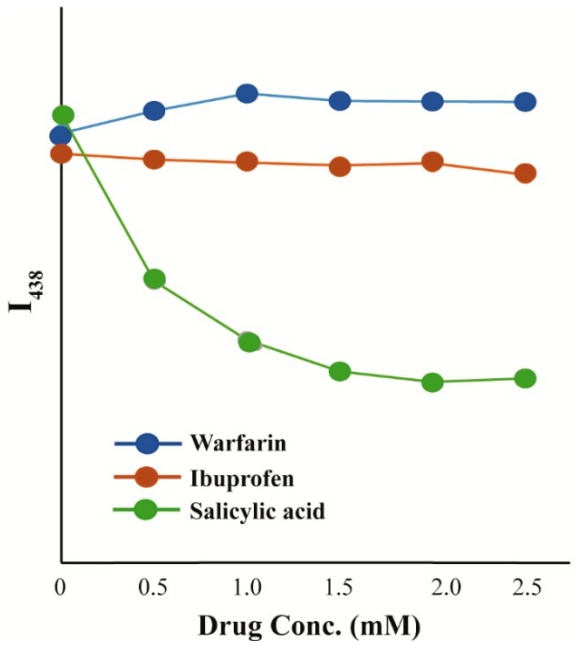

Figure S17: Changes in the emission intensity of $\mathbf{L_1}$ (2 μM) in presence of HSA (150 μg/mL) at 438 nm upon addition of various site specific drugs; λ_{ex}=380 nm.

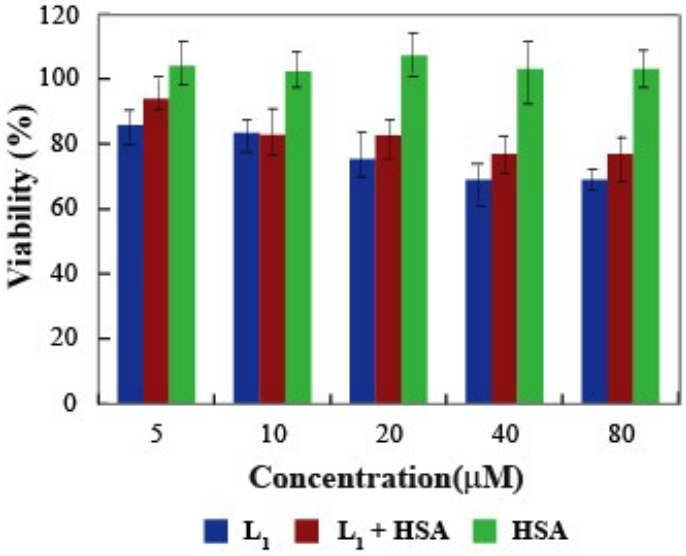

Figure S18: MTT based cytotoxicity assay for (A) probe $\mathbf{L_1}$, $\mathbf{L_1}$/HSA ensemble and (B) only HSA.

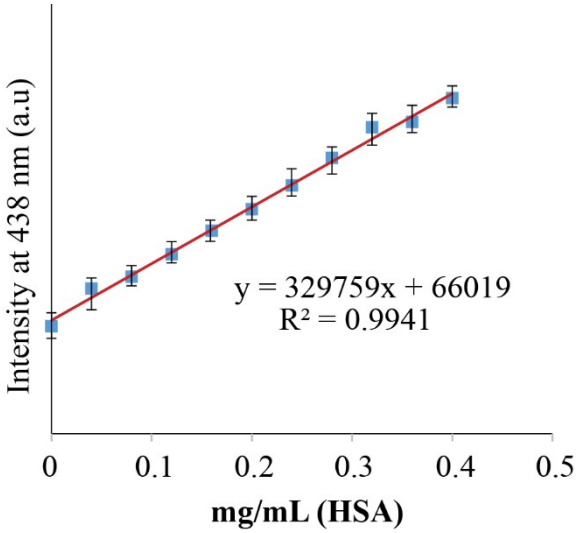

Figure S19: Fluorescence intensity (at 438 nm) vs. concentration of HSA plot for determination of detection limit.

Table S3: Recent progress in the field of HSA sensing, a comparative study.

Sl. No.	Reference	Fluorophoric Receptor type	Solvent system	Detection limit	Analytes detected
1.	Analyst, **2014**, 139, 581–584	Supramolecular aggregates of a cyanine dye	Tris–HCl buffer	Not Reported	Human Serum Albumin
4.	Chem. Commun., **2016**, 52, 6064--6067	2-dicyanomethylene-3-cyano-4,5,5-trimethyl-2,5-dihydrofuran (TCF) derivative	PBS (pH 8)	2.5 mg L1	Human albumin
1.	Sens. Actuators B Chem., **2017**, 243, 831–837	AIE active amphiphilic molecule	Tris-HCl buffer	0.58 g/mL	Human serum albumin and chitosan
3.	Chem. Commun., **2017**, 53, 6432--6435	Coumarin derivative with dioxaborine unit	PBS buffer	0.21 mg/ mL	HSA and BSA
6.	Dyes and Pigments, **2018**, 152,60–66	Three fluorescent chalcone-based dyes CD1-3	PBS buffer	0.57 mg/L	Human Serum Albumin
	J. Lumin., **2018**, 197, 193–199	Two NIR fluorescence probes, BI-FPI and NTPS-FPI	PBS buffer	0.66 mg/L 2.04 mg/L	Human Serum Albumin and Bovine Serum Albumin
7.	Talanta, **2018**, 185, 568–572	Probe XYQ based on the quinoline ring and indole ring	PBS buffer	0.0033 g/L	Human Serum Albumin (site I binding)
8.	**Present Work**	**Di-substituted Urea**	**Water**	**5 µg/mL**	**Human Serum Albumin**

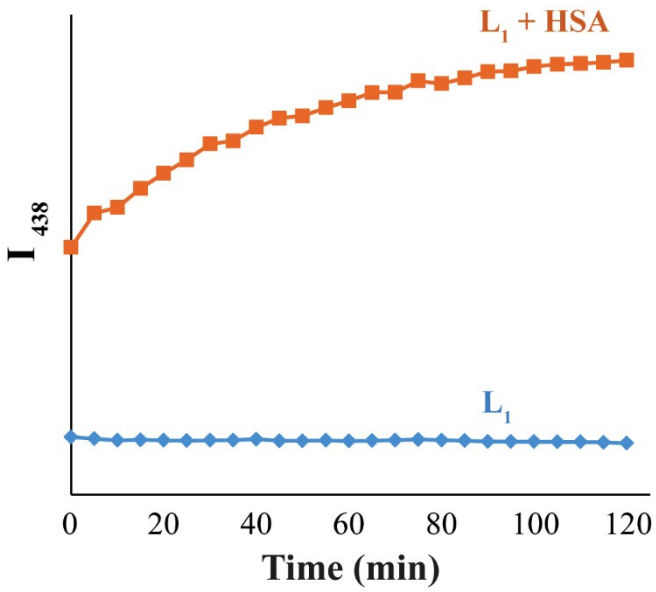

Figure S20: Changes in the emission intensity of $\mathbf{L_1}$ (2 μM) at 438 nm with time upon interaction with HSA (150 μg/mL); λ_{ex}=380 nm.

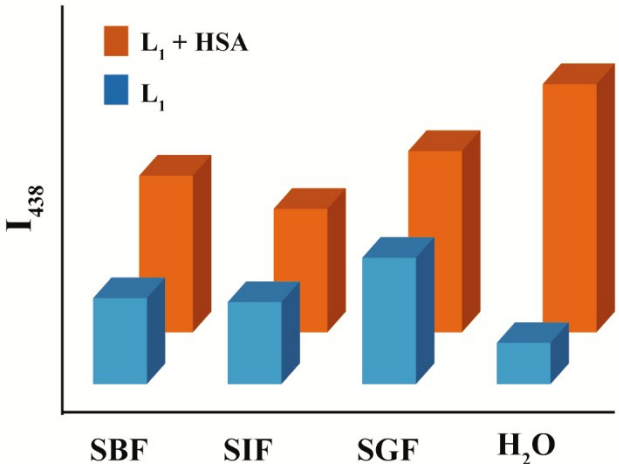

Figure S21: Changes in the emission intensity of $\mathbf{L_1}$ (2 μM) at 438 nm in presence of HSA (150 μg/mL) in bio-fluidic samples [SBF- Simulated Body Fluid (pH~7.4), SIF- Simulated Gastric Fluid (pH~2.0) and SGF- Simulated Intestinal Fluid (pH~8.0)].

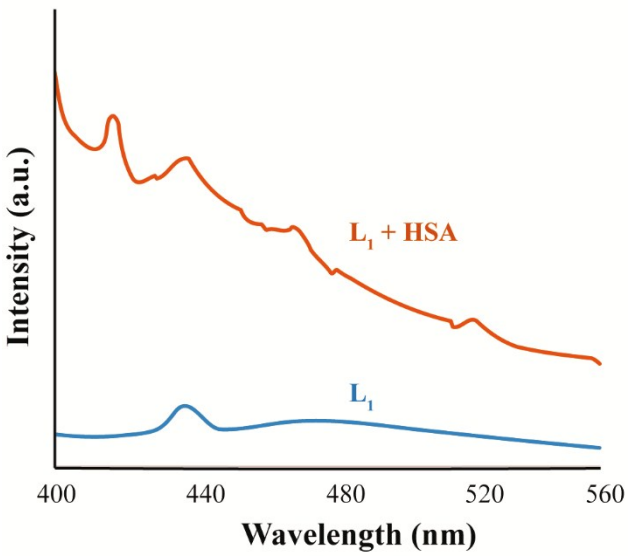

Figure S22: Fluorescence spectra of $\mathbf{L_1}$ (2 μM) in presence of HSA (150 μg/mL) in artificial urine sample.

Hydrophobic Interactions

Index	Residue	AA	Distance	Ligand Atom	Protein Atom
1	210A	ALA	3.26	11277	2029
2	213A	ALA	3.01	11264	2060
3	216A	VAL	3.32	11262	2090
4	327A	LEU	3.42	11261	3134
5	347A	LEU	3.62	11284	3343
6	481A	LEU	3.34	11280	4646
7	482A	VAL	3.10	11280	4654

Figure S23: Interactions encountered in the Docking conformation of HSA/$\mathbf{L_1}$ with the lowest binding free energy obtained from Protein-Ligand Interaction Profiler.